

Geochemical evolution of the Maloin Ranch pluton, Laramie Anorthosite Complex, Wyoming: Trace elements and petrogenetic models

ALLAN KOLKER,* D. H. LINDSLEY, G. N. HANSON

Department of Earth and Space Sciences, State University of New York at Stony Brook,
Stony Brook, New York 11794, U.S.A.

ABSTRACT

The Maloin Ranch pluton is a layered composite intrusion at the southeast margin of the main body of the Laramie Anorthosite. The layering defines a body shaped like a half bowl, which contains ferrodiorite at its base, overlain progressively by fine-grained monzonite and porphyritic monzonite, monzosyenite, and porphyritic granite. The trace element data presented here, together with isotopic data for these rocks (Kolker, 1989) show that each of the members of this composite intrusion has a separate origin. Field, geochemical, and isotopic evidence are consistent with a comagmatic relation between ferrodiorite and anorthositic rocks, either by fractionation or immiscibility. The fine-grained monzonite is not the result of fractionation of ferrodiorite, or mixing of ferrodiorite with a more evolved magma, such as monzosyenite or granite. Trace-element data for the fine-grained monzonite suggest an independent deep-crustal source that was depleted in some incompatible elements.

At intermediate levels in the intrusion, porphyritic monzonite formed by mixing of fine-grained monzonite (or biotite gabbro) and monzosyenite magmas, not by fractionation of the fine-grained monzonite (Kolker and Lindsley, 1989). Textures, REE patterns, and other trace-element data show that the monzosyenite is a feldspar cumulate, with a highly variable proportion of liquid. Trace-element and isotopic characteristics of the Maloin monzosyenite are consistent with derivation from a more evolved deep crustal source or more extensive fractionation, compared to the fine-grained monzonite. REE data suggest that some of the overlying porphyritic granite is a late-stage segregation related to the monzosyenite and not to the overlying Sherman Granite. Associated granitoid dikes and small fine-grained intrusive bodies have a diverse history reflecting late-stage mobility of granitic melts with varying fluid contents.

INTRODUCTION

Evolved rocks ranging from ferrodiorite to granite are found at the margins of most Proterozoic anorthosites (e.g., Morse, 1982; Duchesne, 1984; Emslie, 1985). In the Laramie Anorthosite Complex, examples include the Maloin Ranch pluton and the Sybille pluton, which bound the main anorthositic mass to the southeast and northwest, respectively (Fig. 1). Although considerable progress has been made toward understanding the origin of various anorthosite complexes over the last decade, there remains no consensus on the petrogenesis of the ferrodiorite-ferrosyenite portion of the evolved series.

The debate on the origin of these rock types has centered on the relative importance of crustal anatexis versus fractionation of anorthosite residual liquids. For the ferrodioritic rocks, their proximity to anorthosite bodies, their major element compositions (enriched in Fe, Ti,

and P), and their modest negative europium anomalies have led many workers to suggest these are residual liquids derived from fractionation of plagioclase-rich magmas (Ashwal and Siefert, 1980; Wiebe, 1980, 1984; Wiebe and Wild, 1983; Morse, 1981, 1982). Trace-element data, particularly high Sr concentrations (e.g., 400–500 ppm), and in some cases, lack of negative europium anomalies, have led others to propose modes of origin that are independent of the anorthositic series. These models include melting of mafic lower crust (Duchesne et al., 1985a, 1985b, 1989) and fractionation of mafic magmas that are unrelated to the anorthositic series (Emslie, 1980).

The syenitic rocks have been explained by a similar range of models. Fountain et al. (1981) suggested that syenites in the Sybille body, at the northwest margin of the Laramie Anorthosite, formed by crustal anatexis, whereas Fuhrman et al. (1988) proposed a continuous fractionation series from the anorthosite. In most anorthosite complexes, associated granitic bodies probably represent crustal melts (Anderson, 1983, 1987), although minor granitic segregations may also form by immiscibility (Wiebe, 1979).

* Present address: Department of Applied Science, Brookhaven National Laboratory, Building 815, Upton, New York 11973, U.S.A.

The purpose of this paper is to evaluate petrogenetic models for the ferrodiorite-monzosyenite suite and associated granitic rocks, primarily using major- and trace-element data (including REE) for the Maloin Ranch pluton and more limited data for the Sybille pluton. Corresponding Nd and Sr isotopic data (Kolker, 1989) show similar ranges for the ferrodiorite and associated anorthositic rocks, suggesting a comagmatic relation. The fine-grained monzonite has more primitive isotopic characteristics (lower I_{Sr} , higher ϵ_{Nd}) than do the anorthosite and ferrodiorite, which is inconsistent with the evolution of fine-grained monzonite by fractionation of ferrodiorite (Fuhrman et al., 1988), mixing of ferrodiorite and monzosyenite (Kolker et al., 1988), or progressive contamination of ferrodiorite by melts from lower Proterozoic country rock.

In this paper, the available Sr and Nd isotope data are considered together with major- and trace-element data in developing petrogenetic models for the ferrodiorite-granite series. This paper is the companion to a field and petrologic investigation of the Maloin Ranch pluton (Kolker and Lindsley, 1989). The Maloin Ranch pluton presents a particularly good opportunity to study the evolved suite because the characteristic range in rock types is present in a well-defined stratigraphy, and has not been subjected to post-emplacement metamorphism.

The range of rock types in the Maloin Ranch pluton (ferrodiorite to granite) is similar to that present in the Sybille pluton to the northwest (Fuhrman et al., 1988), but the Sybille body lacks a clearly defined stratigraphy. Field relations, petrography, mineral chemistry, and crystallization conditions in the Maloin Ranch pluton and Sybille pluton are discussed at length by Kolker and Lindsley (1989) and by Fuhrman et al. (1988), respectively.

GEOLOGIC AND PETROLOGIC SETTING

Mid-Proterozoic rocks of the Laramie Anorthosite Complex were emplaced across the projected trace of the Cheyenne Belt, a prominent northeast-trending discontinuity separating the Archean Wyoming Province on the north side of the belt from early Proterozoic basement to the south (Hills and Houston, 1979; Karlstrom and Houston, 1984; Duebendorfer and Houston, 1987; Geist et al., 1989). The Maloin Ranch pluton intrudes along the southeast margin of the main anorthositic body in the Laramie Anorthosite Complex (Fig. 1). The composite pluton includes ferrodiorite at its base, overlain progressively by fine-grained monzonite and porphyritic monzonite, monzosyenite, and, at the top of the intrusion, porphyritic granite (Fig. 2). Throughout the entire stratigraphy, dikes and small intrusive bodies of fine-grained granitoids crosscut other rock types. Biotite gabbro is present locally, occurring as minor conformable or cross-cutting bodies.

Contact relationships between units within the Maloin Ranch pluton range from sharp intrusive contacts to gradational contacts and heterogeneous zones of magma

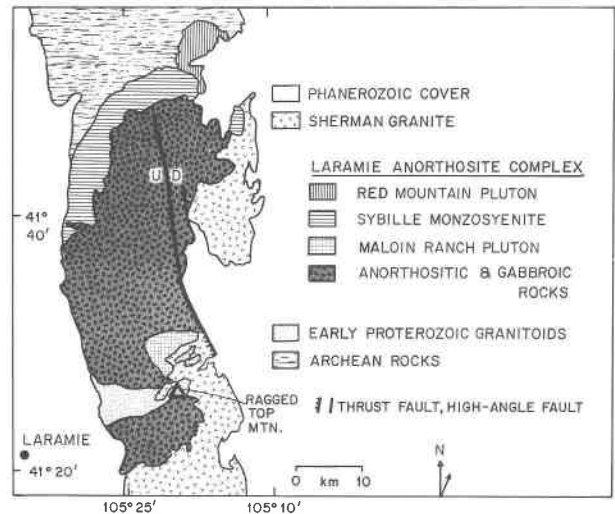


Fig. 1. Geologic location map of the Laramie Anorthosite Complex and surrounding rocks, southeastern Wyoming.

mixing. Ferrodiorite is restricted to the anorthosite contact and to minor occurrences within anorthositic rocks near the contact. The transition from ferrodiorite to fine-grained monzonite appears to be gradational over a lateral distance of several hundred meters. Contacts between fine-grained monzonite and monzosyenite are generally sharp, except in a zone approximately 250 m thick, where chilled bands of fine-grained monzonite and biotite gabbro locally mixed with a monzosyenite host magma, forming the heterogeneous porphyritic monzonites (Kolker and Lindsley, 1989). These mixing relations show that at least part of the ferrodiorite-to-monzosyenite series is not a result of continuous fractionation of ferrodioritic magma, a model suggested by Fuhrman et al. (1988) for the Sybille pluton.

In the upper portion of the Maloin Ranch pluton, monzosyenite grades upward into porphyritic granite through a quartz syenite member. The coarsest porphyritic granites, found at the southeast corner of the study area, contain tabular microcline megacrysts and resemble portions of the Sherman Granite.

Progressive increases in $Fe/(Fe + Mg)$, where Fe is total Fe as Fe^{2+} , and alkali enrichment are apparent with height in the Maloin Ranch pluton, with corresponding variation in the compositions of pyroxenes, olivines, feldspars, and other minerals (Kolker and Lindsley, 1989). Compositions of plagioclase and pyroxene in Maloin Ranch ferrodiorite overlap with those in anorthositic rocks but trend to more evolved compositions. In porphyritic monzonite, plagioclase, pyroxene, and olivine compositions are intermediate between fine-grained monzonite and monzosyenite compositions where these magmas mixed. Where a larger portion of biotite gabbro mixed with monzosyenite, pyroxenes in porphyritic monzonite trend toward much more magnesian compositions (Kolker and Lindsley, 1989; Fig. 10). Near the top of the Maloin Ranch pluton, an increasing fluid component is re-

plutons and in the surrounding Sherman Granite. Zircons in Maloin Ranch and Sybille monzosyenites give concordant U-Pb ages of 1430 ± 15 Ma (Subbarayudu et al., 1975; R. E. Zartman, personal communication, 1987). Zircons in the Red Mountain pluton, which intrudes the Sybille pluton, give a slightly discordant age of $1439 \pm 7/-6$ Ma (Frost et al., 1990). U-Pb ages for zircon from the Sherman Granite are 1430 ± 20 Ma, suggesting that the Sherman Granite may be coeval with the syenitic rocks (Subbarayudu et al., 1975; Aleinikoff, 1983; R. E. Zartman, personal communication, 1987).

The anorthositic rocks have not been dated directly. The presence of anorthositic plagioclase xenocrysts (but lack of anorthosite xenoliths) in fine-grained monzonite, monzosyenite, and biotite gabbro suggest that the anorthosite may not have been completely solidified when the Maloin Ranch pluton was emplaced. Within the Maloin Ranch layered zone, mutual injection of biotite gabbro, fine-grained monzonite, and monzosyenite shows that these three magmas were contemporaneous (Kolker and Lindsley, 1989).

ANALYTICAL METHODS

Availability of pristine whole-rock samples for geochemistry was limited by extensive weathering in the study area. Most of the large whole-rock samples were extracted from the outcrop using 1.25-inch diameter wedge-and-feather sets, which were inserted into holes drilled by a gasoline-powered drill. Additional unweathered samples were obtained in blasted spillways of livestock watering ponds. Representative whole-rock splits were prepared by a sequence of crushing in a steel mortar, mixing on paper, and quartering. This procedure reduced the sample from initial amounts of 2–12 kg to 30–50 g of material having a maximum grain-size of 2–3 mm (Shirey, 1984). These splits were then powdered in a tungsten-carbide vessel, using a motorized shatterbox.

Major elements were determined on fused glass disks by X-ray fluorescence (Norrish and Hutton, 1969) as reported by Kolker and Lindsley (1989). Trace elements (excluding REE) were determined by X-ray fluorescence using pellets pressed from whole-rock powder (method of Norrish and Chappell, 1977), at the University of Massachusetts, Amherst. Estimated precision for XRF analyses is better than 2% of the amount present for Rb, Sr, and Y, and 2–3% of the amount present for most other trace elements, except La, Ba, Ga, U, Th, and Pb (estimated precision ranges from 5–10%). Detection limits are <1 ppm for Rb, Sr, Nb, and Y; 1–2 ppm for Zr, Ga, Th, U, and Pb; 3 ppm for Zn, Ni, Cr, and V; and 5 ppm for Ba and La. W and Co were not determined because of contamination from the WC shatterbox vessel. Nb contributed by the shatterbox vessel is $\leq 1/2$ ppm, for which no correction was made.

Rare earth elements were analyzed by isotope dilution, using the same whole-rock powders as used for the XRF analyses. REE concentrations were determined with the 6-inch (15 cm) radius, 60°-sector Shields-type mass spec-

trometer at Stony Brook. REE were separated using the procedure outlined by Shirey and Hanson (1986), with modifications introduced by Evans (1987; Appendix 1). Sample powders were mixed with lithium-metaborate flux and fused in high-purity graphite crucibles for 15 minutes at 1050 °C. Sample glasses were dissolved in spiked 1 N HNO₃ and the REE were coprecipitated as a group with Fe(OH)₃ and Al(OH)₃, by adding NH₄OH until the solution reached a pH of 6–8. The precipitate was then dissolved by adding 2.0 N HCl. REE were separated into four fractions, using a two-column (HCl, methallactic acid) procedure. Average reproducibility of complete chemical replicates is better than 2% of the amount present for each of the REE analyzed (Kolker, 1989; Appendix 2). Total analytical blanks for Nd are less than 2 ng. Blanks for other REE are extrapolated from the light-REE-enriched pattern for blanks shown by Vocke (1983) and G. N. Hanson (unpublished data). In all cases, blank corrections are negligible. REE patterns are normalized to isotope dilution values for the Leedeey chondrite (Masuda et al., 1973) divided by 1.20 (Hanson, 1980; Table 1).

GEOCHEMISTRY

In this section, major- and trace-element data for Maloin Ranch rock types are presented within the context of corresponding petrogenetic models, to be considered more fully in later sections. The major- and trace-element data for the individual samples are in Table 1. A summary of the geochemical characteristics for each rock type is in Table 2. Major-element characteristics of the Maloin Ranch pluton are typical of the range of evolved rocks at anorthosite margins. As shown by Kolker and Lindsley (1989), in going from ferrodiorite to monzosyenite, SiO₂, Al₂O₃, alkalis, and Fe/(Fe + Mg) increase, while CaO, FeO, MgO, TiO₂, and P₂O₅ decrease. Such trends are the basis for the continuous fractionation model for similar rock types in the Sybille pluton (Fuhrman et al., 1988).

Only one ferrodiorite sample was analyzed (RTM 26), but its composition is similar to that of ferrodiorite sample SR 123d (monzogabbro of Fuhrman et al., 1988) from the Sybille pluton. Both ferrodiorite samples have less than 45 wt% SiO₂, and are enriched in TiO₂ (3.9–4.4 wt%), total iron (16.6–25.9 wt%), CaO (8.9–9.9 wt%), and P₂O₅ (2.0–2.6 wt%), consistent with enrichments suggested for anorthosite residual liquids (Ashwal, 1978; Wiebe, 1979; Ashwal and Siefert, 1980; Morse, 1982; Wiebe and Wild, 1983; Goldberg, 1984). In this model, coprecipitation of plagioclase and a phase that excludes Sr (e.g., pyroxene) is required to explain the high Sr concentrations of the ferrodiorite (RTM 26–468 ppm; SR 123d–478 ppm; see section on the origin of ferrodiorite). For RTM 26, Rb (2 ppm), Rb/Sr (0.004) and Zr (57 ppm) are very low, similar to values for the anorthositic rocks. If this ferrodiorite is a crustal melt (e.g., Duchesne et al., 1985a, 1985b, 1989), these values would require a source that is strongly depleted in incompatible elements. The K/Rb ratio of ferrodiorite is the highest of the evolved rocks (1660, RTM 26; 1494, SR 123d), with values similar to high K/Rb

TABLE 1. Major- and trace-element analyses

Maloin Ranch pluton																			
Anorthosite				Ferrochlorite				Fine-grained monzonite				Porphyritic monzonite		Monzosyenite				Biotite gabbro	
RTM 11A	RTM 58	BM 4A	RTM 26	GM 9	GM 15A	GM 12F	GM 12G	GM 27	RTM 35	GM 24	RTM 34B	RTM 46	RTM 35	GM 24	RTM 34B	RTM 46			
SiO ₂	53.93	50.80	44.78	50.41	49.83	55.97	61.80	62.06	62.75	49.83	47.69	48.09	62.75	49.83	47.69	48.09			
TiO ₂	0.26	0.69	4.43	3.18	2.95	1.57	2.92	0.65	0.73	0.96	1.40	1.85	0.73	0.96	1.40	1.85			
Al ₂ O ₃	27.60	20.43	14.06	14.27	14.10	15.39	17.95	17.35	16.81	17.97	17.67	18.37	16.81	17.97	17.67	18.37			
FeO†	1.62	9.48	16.69	14.25	15.31	12.01	5.53	4.89	5.70	10.19	10.85	11.42	5.70	10.19	10.85	11.42			
MnO	0.02	0.13	0.26	0.22	0.22	0.22	0.10	0.09	0.10	0.15	0.23	0.19	0.10	0.15	0.23	0.19			
MgO	0.36	6.05	5.33	3.27	2.92	2.87	0.42	0.51	0.42	8.84	7.71	6.81	0.42	8.84	7.71	6.81			
CaO	10.93	8.37	9.89	7.61	7.33	5.69	3.56	2.64	2.88	8.24	10.65	9.05	2.88	8.24	10.65	9.05			
Na ₂ O	4.50	4.45	2.57	3.47	3.33	3.86	4.76	4.19	4.29	2.74	1.82	3.00	4.29	2.74	1.82	3.00			
K ₂ O	0.63	0.68	0.40	2.17	2.33	2.70	4.43	6.28	5.61	0.83	2.14	0.96	5.61	0.83	2.14	0.96			
P ₂ O ₅	0.09	0.15	2.01	1.25	1.48	0.16	0.18	0.20	0.16	0.16	0.17	0.30	0.16	0.16	0.17	0.30			
Total	99.94	100.23	100.42	100.10	99.83	100.44	99.45	98.86	99.53	99.95	100.33	100.04	99.53	99.95	100.33	100.04			
Mg#‡	0.285	0.532	0.363	0.290	0.254	0.299	0.119	0.157	0.135	0.608	0.558	0.515	0.135	0.608	0.558	0.515			
Trace elements (ppm)																			
V	15	30	300	122	48	147	13	14	13	96	195	170	13	96	195	170			
Cr	3	dl	16	dl	dl	29	3	dl	dl	17	52	51	3	17	52	51			
Ni	109	81	18	14	10	31	7	4	4	189	35	68	4	189	35	68			
Zn	20	78	179	167	197	199	103	98	140	94	100	137	103	94	100	137			
Ga	22	21	23	28	27	27	32	26	29	20	19	22	29	20	19	22			
Rb	3	4	1.96§	26	23	34	51	80	98	14	92	20	98	14	92	20			
Sr	1016	688	468.3§	441	468	309	289	264	264	561	252	641	264	561	252	641			
Y	3	4	41	67	69	37	21	25	39	14	23	14	39	14	23	14			
Zr	20	19	57	605	363	531	939	715	825	102	103	55	825	102	103	55			
Nb	1	2	19	41	41	28	21	23	51	8	6	8	51	8	6	8			
Ba	422	445	445	1523	1717	947	1715	2182	1961	401	262	444	1961	401	262	444			
La	dl	6	37	78	65	38	37	45	54	10	9	16	54	10	9	16			
Ce§	8.95	13.79	84.43	165.9	157.3	87.13	70.41	75.33	106.35	28.71	29.03	24.32	106.35	28.71	29.03	24.32			
Nd§	4.46	7.15	54.69	91.77	92.96	45.54	35.78	39.50	57.73	15.10	16.22	14.82	57.73	15.10	16.22	14.82			
Sm§	0.853	1.44	11.71	18.89	19.58	9.68	6.73	7.83	12.29	3.26	3.90	3.40	12.29	3.26	3.90	3.40			
Eu§	1.07	1.53	3.42	4.73	5.80	2.67	4.36	3.82	3.67	1.18	1.36	1.67	3.67	1.18	1.36	1.67			
Gd§	0.761	1.03	11.23	17.34	17.87	9.21	5.93	7.10	11.01	3.07	4.26	3.42	11.01	3.07	4.26	3.42			
Dy§	0.553	0.739	8.21	13.96	14.04	7.93	4.40	5.49	8.90	2.76	4.40	2.89	8.90	2.76	4.40	2.89			
Er§	0.264	0.350	3.90	6.92	6.94	4.39	2.31	2.89	4.60	1.50	2.58	1.46	4.60	1.50	2.58	1.46			
Yb§	0.203	0.453	2.91	5.85	5.52	4.13	2.10	2.57	4.03	1.34	2.32	1.19	4.03	1.34	2.32	1.19			
Pb	3	2	6	13	11	16	17	20	22	6	6	5	22	6	6	5			
Th	dl	dl	dl	dl	dl	4	dl	dl	3	dl	dl	dl	3	dl	dl	dl			
U	2	dl	—	dl	dl	—	—	—	—	—	—	—	—	—	—	—			
SiO ₂	47.27	68.40	75.93	75.46	86.07	39.13	49.38	51.38	47.95	50.58	53.94	61.79	47.95	50.58	53.94	61.79			
TiO ₂	2.08	0.50	0.01	0.08	0.25	3.80	2.62	1.84	2.41	2.49	1.97	0.67	2.41	2.49	1.97	0.67			
Al ₂ O ₃	18.08	15.70	13.34	13.30	5.77	11.18	13.65	16.49	14.38	14.81	14.63	16.94	14.38	14.81	14.63	16.94			
FeO†	12.35	3.21	0.43	0.86	1.37	25.26	17.90	13.57	18.23	15.09	14.20	6.10	18.23	15.09	14.20	6.10			

TABLE 1—Continued

Biotite gabbro	Maloin Ranch pluton						Sybille pluton								
	Granite			Granitic dikes			Ferrochlorite			Fine-grained monzonite			PMZ monzoniyenite		
	RTM 47	RTM 56	GM 23	RTM 32	GM 15B	RTM 43*	SR 123d**	LAC 6A	GR 52	GR 89	PM 45A	PM 103	LAC 9		
MnO	0.19	0.02	0.05	0.00	0.03	0.03	0.45	0.27	0.20	0.27	0.22	0.25	0.13		
MgO	7.06	0.09	0.87	0.03	0.12	0.20	3.70	2.25	1.55	1.98	2.63	1.83	0.39		
CaO	9.30	0.72	2.45	0.29	0.79	0.52	8.70	6.75	7.10	6.94	6.41	6.28	3.25		
Na ₂ O	3.00	2.77	3.38	3.63	3.26	0.04	2.14	3.62	3.97	3.27	3.51	4.14	4.09		
K ₂ O	0.41	5.40	4.75	5.90	5.42	4.36	0.70	2.38	2.62	2.42	3.00	1.99	5.63		
P ₂ O ₅	0.32	0.02	0.15	0.00	0.02	0.05	2.55	1.33	1.17	1.32	1.38	0.96	0.19		
Total	100.06	99.49	99.46	99.56	99.34	98.66	97.61	100.15	99.89	99.17	100.12	100.19	99.18		
Mg# [†]	0.505	0.126	0.326	0.105	0.200	0.208	0.207	0.183	0.169	0.162	0.237	0.187	0.102		
Trace elements (ppm)															
V	175	dl	41	dl	6	21	61	37	23	31	77	29	4		
Cr	51	dl	11	dl	dl	6	6	dl	dl	dl	dl	dl	dl		
Ni	70	dl	9	dl	dl	9	21	9	5	6	5	7	7		
Zn	149	27	61	12	22	38	249	209	172	206	213	164	115		
Ga	20	19	19	33	16	5	26	26	29	28	25	27	29		
Rb	2	95	169	335	202	87	4	14	27	28	37	25	84		
Sr	652	65	278	4	126	58	478	441	543	467	445	542	306		
Y	13	7	31	15	13	51	53	47	39	41	42	39	35		
Zr	44	90	281	45	96	303	166	299	297	94	479	310	791		
Nb	7	6	18	6	11	23	34	40	26	33	38	26	39		
Ba	287	429	1048	6	800	2451	662	2284	2748	3517	3013	1518	2537		
La	6	14	120	9	14	33	63	59	55	52	68	42	47		
Ce ₂	20.92	27.90	183.3	32.90	36.55	77.72	—	135.3	121.7	127.2	—	109.2	117.0		
Nd ₂	13.48	11.11	67.16	5.36	13.95	39.98	—	77.77	70.96	74.88	—	65.01	61.81		
Sm ₂	3.18	2.06	10.82	1.76	2.77	7.98	—	15.85	14.39	15.17	—	13.57	12.17		
Eu ₂	1.62	1.88	1.34	0.043	0.592	1.24	—	5.08	6.34	6.10	—	4.21	5.19		
Gd ₂	3.20	1.73	7.92	1.50	2.15	7.98	—	14.14	12.51	13.07	—	12.29	10.34		
Dy ₂	2.69	1.49	6.22	3.09	1.88	8.85	—	10.34	8.63	8.94	—	8.65	8.02		
Er ₂	1.34	0.785	3.26	2.85	1.20	6.02	—	4.87	3.86	3.98	—	4.02	3.92		
Yb ₂	1.05	0.713	2.75	4.73	1.25	5.76	—	3.90	2.90	2.99	—	3.16	3.65		
Pb	8	17	20	50	22	12	9	17	14	11	13	17	21		
Th	—	3	28	6	21	5	2	dl	2	2	3	dl	5		
U	—	—	—	9	—	—	—	dl	dl	dl	—	dl	5		

Note: dl = at or below detection limit, — = not determined.

* From shear zone.

** Major element data for SR 123d from Fuhrman et al. (1988).

† Total Fe as FeO.

‡ Mg number calculated with all Fe as FeO.

§ Indicates analyses by isotope dilution; all other data by X-ray fluorescence.

TABLE 2. Selected geochemical characteristics, Maloin Ranch pluton

	Anorthosite	Biotite gabbro*	Ferrodiorite**	Fine-grained monzonite	Monzosyenite	Granitic dikes†
SiO ₂	51–54	47–50	<45	49.9–50.4	62–63	69–76
Na ₂ O + K ₂ O	4.1–5.2	3.4–4.0	2.9–3.0	5.6–5.7	9.2–10.6	8.2–9.6
Mg#	0.28–0.53‡	0.51–0.61	0.21–0.36	0.25–0.29	0.12–0.16	0.11–0.33
K/Rb	875–2010	400–1700*	1500–1660	690–840	480–730	147–235
Rb/Sr	0.003–0.008	0.003–0.030*	0.004–0.008	0.05–0.06	0.18–0.37	0.61–83.8
Ce/Zr	0.45–0.76	0.28–0.48	0.9–1.5	0.27–0.43	0.08–0.13	0.38–0.73
Ce/Yb _N	7.8–14.0	5.1–5.5*	7.5	7.2–7.3	6.8–8.6	1.8–17.1
Ce/Nd _N	1.42–1.58	1.1–1.4	1.13	1.24–1.33	1.35–1.45	1.9–4.5
Eu/Eu†	3.4–4.1	1.0–1.6	0.92	0.81–0.96	0.97–2.13	0.08–0.75
ε _{Nd} (1440)	–0.1––1.4	2.2–1.5	–0.6––0.8	0.8–0.4	–1.4––1.6	–0.6––3.9
I _{Sr} (1440)	0.7042–0.7058§	0.7033	0.7051–0.7057	0.7039 ¹	0.7075	0.7076 ¹

* Where indicated, biotite gabbro ranges exclude extreme values for sample RTM 34B, an inclusion(?) in porphyritic granite.

** Where ranges are indicated, FDI data include analyses for Sybille sample SR 123d.

† Ranges for granitic dikes exclude sample RTM 43, collected from a shear zone.

‡ Low whole-rock Mg number for some anorthosites reflects presence of Fe-Ti oxides.

§ Higher values of I_{Sr} reflect values for anorthositic rocks to the north of the Maloin Ranch pluton (Geist et al., 1990; Goldberg, 1984).

|| Sr initial values for only one sample.

ratios of anorthositic rocks surrounding the Maloin Ranch pluton (876–2011; Table 2).

Fine-grained monzonite is also enriched in Fe, Ti, Ca, and P, although this enrichment is less extreme. Mg number for the Maloin Ranch fine-grained monzonite (0.254, 0.290, calculated with all Fe as FeO) is lower than that for the Maloin Ranch ferrodiorite (0.363). Concentrations of incompatible elements (Rb, Zr, Ba, Pb, K) are enriched by up to 10 times those in ferrodiorite (Table 1). If the monzonite were derived by fractional crystallization from the ferrodiorite, these enrichments would require 90% fractional crystallization. Like the ferrodiorite, Sr concentrations of the fine-grained monzonite are high (441–468 ppm). Values for Rb/Sr (0.032–0.109) and K/Rb (665–1388) are not as extreme as those of the ferrodiorite (Table 2).

The monzosyenite is alkalic (Na₂O + K₂O = 9 to 10.5 wt%), with low Mg numbers (ca. 0.1), and intermediate SiO₂ contents averaging about 62 wt%. Concentrations of Rb (50–100 ppm) and Zr (700–950 ppm) are substantially enriched versus fine-grained monzonite, and together with the low Mg numbers suggest a more evolved source, or very large extents of fractionation. Other incompatible element concentrations (e.g., Ba, ca. 2000 ppm; Nb, 20–50 ppm) are similar to values for fine-grained monzonite; Y and REE concentrations are lower in monzosyenite than in Maloin Ranch fine-grained monzonite (Table 1). Values for K/Rb (480–730) and Rb/Sr (0.175–0.369) are more moderate in monzosyenite than in fine-grained monzonite (Table 2).

Granitic rocks show considerable compositional variation in the Maloin Ranch pluton, suggesting a diverse history. With the exception of GM 23, all of the Maloin granites have SiO₂ contents greater than 75 wt% and are mildly peraluminous. Trace-element characteristics are highly variable, with Rb/Sr ranging from 0.607 (GM 23) to 83.8 (RTM 32; Table 2).

Biotite gabbro is the least-evolved rock in the Maloin Ranch pluton, with Mg numbers ranging from 0.50 to

0.60. Cr (17–52 ppm) and Ni (70–189 ppm) are higher in biotite gabbro than in rocks of the ferrodiorite-monzosyenite series (Table 1). The Cr and Ni values, and the intermediate Mg numbers, are well below values for primary melts of the mantle, but may reflect subsequent fractionation of mantle-derived melts, as suggested by their relatively primitive isotopic signatures (Kolker, 1989; Table 2).

Rare earth elements

Because plagioclase fractionation strongly controls the distribution of divalent europium in magmatic systems, previous studies have focused on the presence or absence of negative europium anomalies in interpreting the relation of evolved rocks to associated anorthosites (e.g., Ashwal and Siefert, 1980; Duchesne et al., 1985a, 1985b, 1989). The fact that large negative europium anomalies are uncommon even in ferrodiorites suggests that if plagioclase fractionation had occurred, it must have been offset by fractionation of phases that have negative Eu anomalies in their mineral-melt distribution patterns (e.g., clinopyroxene, apatite; see section on the origin of ferrodiorite).

Anorthositic rocks surrounding the Maloin pluton have LREE-enriched patterns (Ce/Yb_N = 7.8–14.0), large positive europium anomalies (Eu/Eu* = 3.4–4.1), and high Sr concentrations (688–1016 ppm) typical of plagioclase cumulates (Fig. 3). REE patterns for the ferrodiorite-monzosyenite suite show consistent moderate-to-strong LREE enrichment (Ce/Yb_N = 6.8 to 8.6; Fig. 3, 4). REE distribution for the ferrodiorite (sample RTM 26) shows a small negative Eu anomaly (Eu/Eu* = 0.92), and compared to fine-grained monzonite and monzosyenite, a slight depletion of Ce relative to the MREE (Ce/Nd_N = 1.13; Fig. 3). Several Sybille ferrodiorites have higher REE abundances than does RTM 26, with larger negative Eu anomalies (D. H. Lindsley, unpublished data).

REE patterns for fine-grained monzonite (Fig. 3) are similar to those for RTM 26, with up to two times higher

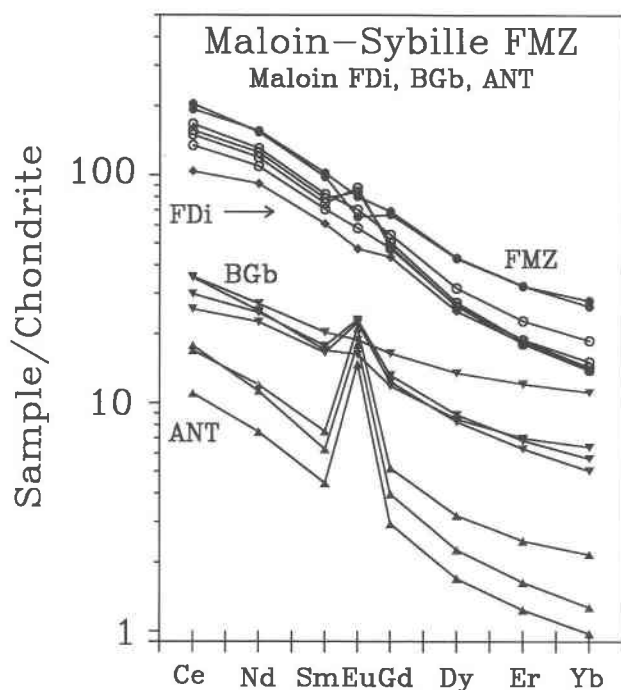


Fig. 3. Chondrite-normalized REE data for Maloin Ranch pluton (solid symbols) and Sybille pluton fine-grained monzonite (open circles). Maloin Ranch data include fine-grained monzonite (circles), ferrodiorite (diamonds), biotite gabbro (inverted triangles) and anorthositic rocks (triangles).

concentrations and a variable europium anomaly that is not correlated with an Mg number. One fine-grained monzonite has a larger negative Eu anomaly ($\text{Eu}/\text{Eu}^* = 0.81$) than does ferrodiorite RTM 26. Positive europium anomalies were observed in two fine-grained monzonite samples from the Sybille pluton. Similar variations in Eu anomaly have been observed in monzonorites (equivalent to ferrodiorite and fine-grained monzonite) of the Rogaland Complex (Duchesne et al., 1985a, 1989).

REE patterns for Maloin Ranch biotite gabbros have abundances that are an order of magnitude lower than those for the ferrodiorite-monzosyenite series and are less enriched in LREE ($\text{Ce}/\text{Yb}_N = 3.20\text{--}5.50$; Fig. 3). Three of the four biotite gabbros have a positive Eu anomaly. No other textural or geochemical evidence indicates that the biotite gabbros are cumulates, and we suspect that the Eu anomaly is a primary characteristic of the melt.

REE patterns for Maloin Ranch monzosyenite are nearly parallel, with two samples (GM 27 and GM 12G) showing substantial positive europium anomalies, consistent with feldspar accumulation (Fig. 4). Feldspar accumulation is also suggested by high modal feldspar abundances (e.g., sample GM 27 consists modally of more than 85% plagioclase + potassium feldspar; Kolker and Lindsley, 1989). Sample RTM 35 has the highest REE and incompatible element concentrations (with the exception of Zr, which is the second highest at 825 ppm),

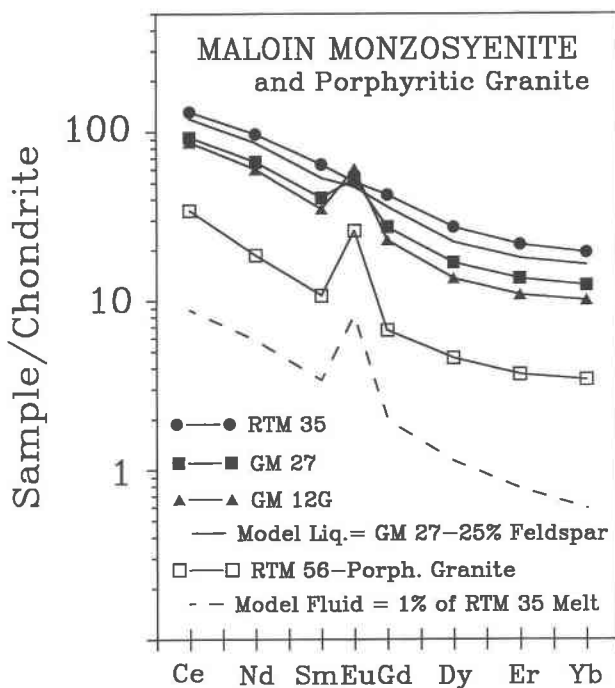


Fig. 4. Chondrite-normalized REE plot for Maloin Ranch monzosyenite (solid symbols keyed to samples) and Maloin Ranch porphyritic granite sample RTM 56 (open squares). Solid line represents the REE distribution of a model liquid produced by subtracting 25% cumulus feldspar from monzosyenite sample GM 27. Feldspar-melt K_d values are from Hanson (1980; Table 2). Also shown is REE distribution for model fluid making up 1% of a monzosyenite melt having the composition of sample RTM 35 (dashed line). Fluid-melt K_d values are from Flynn and Burnham (1978), interpolated for some REE.

and lacks a europium anomaly. This suggests that RTM 35 has the lowest proportion of cumulus feldspar, a finding supported by covariation of K/Rb , Rb/Sr , Ce/Nd , Ce/Yb , and some incompatible element concentrations with europium anomaly (Fig. 5). A model liquid having an REE pattern similar to that of RTM 35 can be generated by subtracting 25% cumulus feldspar ($\frac{2}{3}$ alkali-feldspar, $\frac{1}{3}$ plagioclase) from sample GM 27, a more typical monzosyenite (Fig. 4). The small range of Eu contents for the natural samples suggests a feldspar-melt K_d of about one and a melt whose Eu content was similar to that of RTM 35. Monzosyenite REE patterns show a pronounced flattening in the heavy REE, a characteristic shown to a much lesser extent by Maloin Ranch fine-grained monzonite, but not observed in ferrodiorite RTM 26.

The REE pattern for sample RTM 56, taken from a small segregation of medium-grained porphyritic granite that caps the monzosyenite body of sample RTM 35, is similar to that for the monzosyenite, but with abundances lower by an order of magnitude, and large positive Eu anomaly ($\text{Eu}/\text{Eu}^* = 3.1$; Fig. 4). Compared to the monzosyenite, this granite is highly enriched in silica (77 wt%), and has Sr (65 ppm) and Ba (429 ppm) concentrations

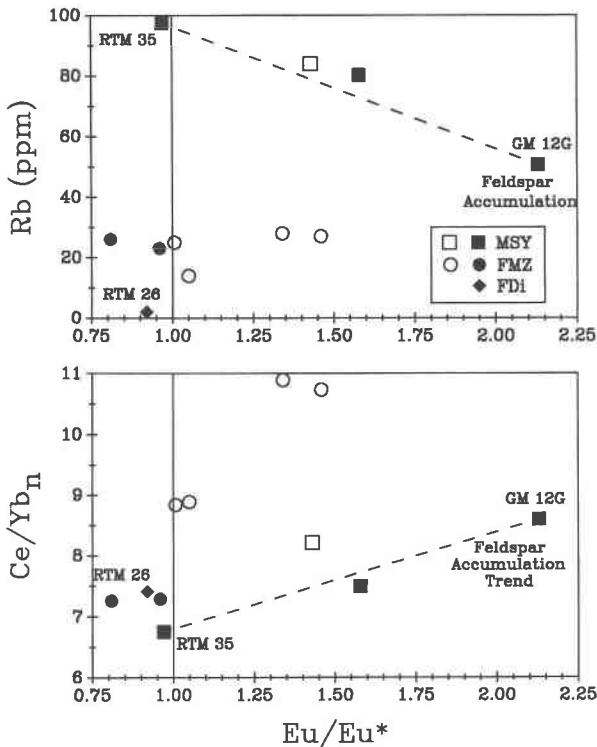


Fig. 5. Plot of Rb concentration (top) and Ce/Yb_N (bottom) versus europium anomaly (Eu/Eu^*) for Maloin Ranch (filled symbols) and Sybille (open symbols) samples including monzosyenite (squares), fine-grained monzonite (circles), and Maloin Ranch ferrodiorite (filled diamond). For monzosyenite, plot shows covariation trends consistent with inferred feldspar accumulation from a near-liquid composition (sample RTM 35). Positive europium anomaly of some Sybille fine-grained monzonites may also be due to accumulation of feldspar.

that are much lower. The lower REE concentrations and silica enrichment each suggest that RTM 56 did not form by fractionation of the monzosyenite. Late-stage granitic differentiates are typically REE-enriched relative to the parent magma; the REE depletion of RTM 56 would require removal of a phase or assemblage with very large mineral-melt K_d values for the REE. The silica enrichment in RTM 56 requires crossing of the quartz-orthoclase cotectic in the haplogranite system in going from monzosyenite to granite (Fig. 6). The low Sr concentration of RTM 56 indicates that feldspar accumulation (suggested by the Eu anomaly) from a melt like monzosyenite RTM 35 (Sr = 264 ppm) was not likely.

REE distribution and other characteristics of RTM 56 may be explained by an increasing water component toward the top of the Maloin pluton (Kolker and Lindsley, 1989). Using the data for partitioning of REE between aqueous fluid and silicate melt for granitic compositions (Flynn and Burnham, 1978), REE distribution is shown for a model hydrothermal fluid representing 1% of a monzosyenite melt having the composition of sample RTM 35 (Fig. 4). A granite that crystallizes from this fluid should

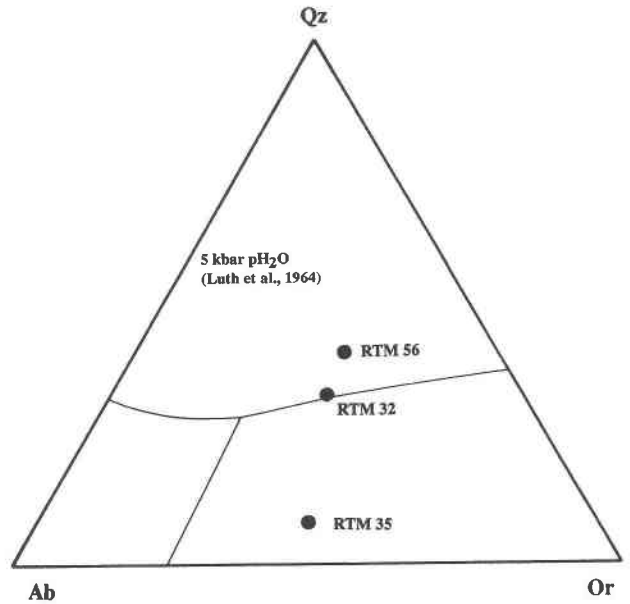


Fig. 6. Ab-Or-Qz ternary diagram showing weight-normative compositions of monzosyenite and granites discussed in text. Samples include inferred near-liquid monzosyenite (RTM 35), associated medium-grained porphyritic granite (RTM 56), and an aplite dike (RTM 32). Phase relations are for the water-saturated, anorthite-absent system at 5 kbar (Luth et al., 1964).

have REE concentrations that are intermediate between those of the fluid and those of the parent melt, as found for sample RTM 56. The low Sr and Ba contents in RTM 56 can be explained by fractional precipitation of granite from the fluid, requiring about 5% crystallization for the RTM 35 model fluid, or less for a siliceous fluid derived from a more-evolved melt (with lower Sr and Ba), assuming feldspar-fluid K_d values for Sr and Ba are very large (Carron and Lagache, 1980). Trace-element data for quartz syenites are needed to understand more fully the monzosyenite to porphyritic granite transition; however, the shape of the REE pattern for RTM 56 suggests that some porphyritic granites in the Maloin Ranch pluton are related to the monzosyenite and not to the overlying Sherman Granite (compare Sherman Granite REE data of Geist et al., 1989).

REE patterns and abundances for the fine-grained granitoids show considerable variation, but each has a negative europium anomaly (Fig. 7). The pattern for an aplitic dike (sample RTM 32) has an extreme europium anomaly and shows downward inflection at Nd (Fig. 7). Such incoherent REE behavior in hydrothermal fluids has been attributed to lanthanide tetrad effects (anomalous behavior associated with $1/4$ -, $1/2$ -, and $3/4$ -filled 4f orbitals; Masuda et al., 1987), or alternatively, to complexing with F or Cl (Mineyev, 1963). Because the REE pattern for sample RTM 32 does not show significant inflection at Gd ($1/2$ -filled) or Er ($3/4$ -filled), the tetrad effect seems unlikely. Normative quartz and feldspar components in RTM 32 correspond closely to cotectic melts in the Ab-

Or-An-Qz-H₂O system, at 5 kbar under water-saturated conditions (e.g., Luth et al., 1964; Nekvasil and Burnham, 1987; Nekvasil, 1988), suggesting that this sample did not crystallize from a fluid (Fig. 6). The REE pattern and bulk composition of RTM 32 could be explained by REE-halogen complexing in a fluid-saturated melt. Nd isotope data for this sample ($\epsilon_{Nd(1440)} = -3.9$) indicate a history of LREE enrichment prior to acquisition of its present Sm/Nd ratio, consistent with an origin by partial melting of lower Proterozoic country rocks.

PETROGENESIS OF THE FERRODIORITE-MONZOSYENITE SERIES

Viable petrogenetic models for the ferrodiorite to monzosyenite series must explain characteristics such as the large range in Mg number and incompatible-element concentrations, the overall LREE enrichment, and the distinct isotopic characteristics for each member of the series. Previous models for the series include (1) partial melting of mafic lower crust and subsequent fractionation at higher levels (e.g., Duchesne et al., 1985a, 1985b, 1989), (2) continuous fractionation of anorthosite residual liquids (e.g., Philpotts, 1966; Fuhrman et al., 1988), and (3) a comagmatic relation between anorthositic rocks and oxide-rich ferrodiorites (this study; Ashwal and Siefert, 1980; Goldberg, 1984), but with associated monzonites, syenites and granites derived by melting of the lower crust (Fountain et al., 1981; McLelland, 1988).

Neither end-member process (models 1 and 2) is satisfactory for the entire Maloin Ranch ferrodiorite-to-monzosyenite series. The crustal-melting model is unlikely for the ferrodiorite because it requires a source that is unreasonably depleted in some incompatible elements (e.g., for sample RTM 26, Rb = 2 ppm, Rb/Sr = 0.004). The presence of small ferrodiorite segregations within the anorthosite is also difficult to explain by the melting model. Although the data are more consistent with a comagmatic relation between anorthosite and ferrodiorite (see below), several factors indicate that the complete ferrodiorite-to-monzosyenite suite is not related by fractionation. Because the exposed volume of monzosyenite is much larger than the ferrodiorite, this model requires huge amounts of ferrodiorite in an undetected magma chamber at depth (Fuhrman et al., 1988). The fractionation model is not supported by isotopic data (Kolker, 1989; Table 2), which require a distinct, isotopically more primitive source for the fine-grained monzonite than that of the anorthosite and ferrodiorite (see section on origin of fine-grained monzonite).

Origin of ferrodiorite

Evidence linking the Maloin Ranch ferrodiorite to the anorthositic rocks includes field relations, continuous plagioclase and pyroxene compositional ranges, major- and trace-element chemistry, and overlapping ranges for Sr and Nd isotopic data (Kolker and Lindsley, 1989; Kolker, 1989; Table 2). Melting experiments suggest that liquids like Sybille ferrodiorite sample SR 123d may co-

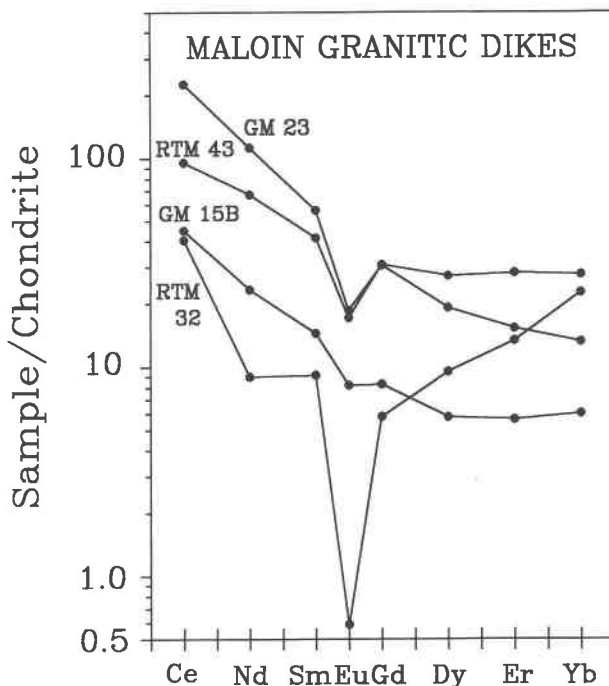


Fig. 7. Chondrite-normalized REE plot for Maloin Ranch granitic dikes.

exist with Fe-Ti-oxide bodies related to the anorthositic rocks of the Laramie Complex (Epler, 1987; Fig. 13).

Despite these indications of a genetic link between anorthosite and ferrodiorite, several features of the ferrodiorites are difficult to explain as part of the anorthositic liquid line of descent. As noted by Emslie (1980) and Duchesne et al. (1985b), the high Sr content of the ferrodiorite is unexpected for a residual liquid left after extensive plagioclase fractionation. A similar argument has been made for the lack of large negative europium anomalies in ferrodiorites (for sample RTM 26 Eu/Eu* is only 0.92). These characteristics may be explained by cotectic crystallization of plagioclase + clinopyroxene in subequal proportions. A residual liquid having a Sr concentration of 480 ppm, near that of ferrodiorite RTM 26 (468 ppm), is consistent with 90% fractionation of a cumulate containing 60% plagioclase, assuming a gabbroic anorthosite parent with 600 ppm Sr (Simmons and Hanson, 1978; Wiebe, 1980) and a mineral-melt K_d of 1.83 for plagioclase (Philpotts and Schnetzler, 1970). The high Sr concentration of the anorthositic plagioclase (1016 ppm for whole-rock anorthosite sample RTM 11A) also suggests that the Sr content of the coexisting liquid was high (e.g., ~500 ppm), if known mineral-melt K_d values are applicable. If substantial pyroxene fractionation is involved, coprecipitation of Fe-Ti oxides is probably required to explain the small shift in Fe/(Fe + Mg) of pyroxenes between anorthosite and ferrodiorite (Kolker and Lindsley, 1989). Other factors which may limit the development of a negative Eu anomaly in the residual liquid

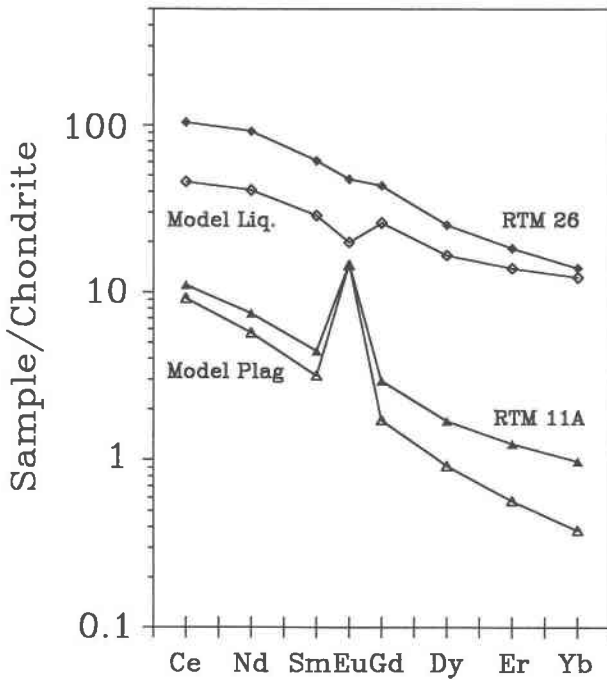


Fig. 8. REE distribution for model intercumulus liquid in anorthositic rocks adjacent to the Maloin Ranch pluton. Calculation assumes anorthosite sample RTM 11A (filled triangles) contains 95% cumulus plagioclase plus 5% model liquid (open diamonds). Model plagioclase (open triangles) is calculated by subtracting 5% model liquid from RTM 11A and is similar to REE data for Laramie plagioclase separates reported by Goldberg (1984). Model liquid is calculated using plagioclase-melt K_d values compiled by Hanson (1980) and the model plagioclase composition. REE distribution of model intercumulus liquid is similar to that of Maloin ferrodiorite RTM 26 (filled diamonds), but with lower abundances.

include (1) an initial positive Eu anomaly of the anorthosite parent (Wiebe, 1980), (2) recharge by successive batches of anorthositic magma, and (3) in the latest stages, crystallization of apatite, as in the Kiglapait intrusion (Morse and Nolan, 1985).

If ferrodiorite sample RTM 26 is an anorthosite residual liquid, mineral-melt K_d values for Rb and K must be much higher than the published values (e.g., Philpotts and Schnetzler, 1970). The low Rb (2 ppm) and K_2O (0.4 wt%) contents of RTM 26 are similar to values expected for a gabbroic anorthosite parent magma. Data on anorthositic plagioclase separates from the Nain Complex (Gill and Murthy, 1970), Marcy massif (Ashwal and Wooden, 1983) and the Kiglapait intrusion (Morse, 1981) indicate plagioclase-melt K_d values for Rb that are higher than expected. The Kiglapait liquid does not reach 2 ppm Rb until 90% solidified (Morse, 1981).

Using REE data for anorthosite sample RTM 11A and plagioclase-melt K_d values (compilation of Hanson, 1980; Table 2), REE distribution was calculated for a model anorthosite liquid composition. The model assumes that RTM 11A consists of 95% cumulus plagioclase and 5%

model intercumulus liquid and that for a given element the composition of the model liquid is defined by $X_{\text{REE(plag)}}(1/K_d)$, where $X_{\text{REE(plag)}}$ is the concentration of an element in the model plagioclase and K_d is the corresponding plagioclase-melt single-element K_d . The model proportions in anorthosite sample RTM 11A were estimated from petrography but also fit the relative P_2O_5 contents in RTM 11A (0.09 wt%) and ferrodiorite RTM 26 (2.01 wt%), assuming that P_2O_5 is only in the liquid.

The calculated intercumulus liquid shows a modest negative europium anomaly ($\text{Eu}/\text{Eu}^* = 0.73$) and distinct flattening in the LREE ($\text{Ce}/\text{Nd}_N = 1.12$), nearly that of ferrodiorite sample RTM 26 ($\text{Ce}/\text{Nd}_N = 1.13$; Fig. 8). The pronounced LREE flattening is consistent with extensive plagioclase fractionation, as suggested by Goldberg (1984) for oxide-rich rocks in Laramie Complex anorthosites to the north. Despite this similarity between RTM 26 and the model liquid, REE concentrations of RTM 26 are probably too high for the liquid from which the anorthositic plagioclase was extracted (for Eu, a plagioclase-melt K_d of only about 0.3 is required).

The possibility remains that RTM 26 and other Laramie ferrodiorites with still higher REE abundances represent later stage fractionates of the intercumulus anorthositic liquid. Some ferrodiorite REE characteristics could also be explained by apatite accumulation (i.e., high abundances, negative Eu anomaly), however, the limited range in P_2O_5 contents and in apatite saturation temperatures suggests that this cannot be a large effect (for RTM 26, $P_2O_5 = 2.01$ wt%, $T_{\text{ap}} = 1000$ °C; for SR 123d, $P_2O_5 = 2.55$ wt%, $T_{\text{ap}} = 970$ °C; Harrison and Watson, 1984).

Problems posed by the fractionation model lead us to consider an additional model for the Maloin Ranch ferrodiorite. Compositions of the Fe-rich ferrodiorites have some characteristics of low-silica immiscible melts produced in experimental studies (e.g., Roedder, 1951, 1978; Watson, 1976; Ryerson and Hess, 1978, 1980) and observed as melt inclusions (Philpotts, 1982). Unlike in these examples, an appropriate felsic conjugate melt is lacking for the Maloin Ranch ferrodiorite. Compared to the ferrodiorite, the more felsic fine-grained monzonite and monzosyenite show enrichment in Zr and have similar (monzosyenite) or higher (fine-grained monzonite) REE concentrations. Previous work shows that both Zr and REE strongly favor the lower-silica melt in immiscible pairs (e.g., Watson, 1976; Ellison and Hess, 1989). Systematic differences in mineral chemistry in the Maloin pluton (Kolker and Lindsley, 1989) are also difficult to explain if ferrodiorite is related to more evolved rocks by immiscibility.

Mineral chemistry of Maloin Ranch ferrodiorite is more consistent with immiscibility between anorthosite and ferrodiorite, as compositions of plagioclase and pyroxenes in the ferrodiorite approach compositions in nearby anorthositic cumulates. Anorthositic and ferrodioritic plagioclases actually show minor overlap at about An_{50} (Kolker and Lindsley, 1989). If anorthosite and ferrodiorite are related by fractionation, the similar compo-

sitions of cumulus and liquid plagioclases require considerable narrowing of the plagioclase two-phase field, compared to the pure system.

Origin of fine-grained monzonite

Sr and Nd isotopic data (Kolker, 1989; Table 2) suggest that fine-grained monzonite is not related to ferrodiorite by closed-system fractionation. Likewise, these data show that fine-grained monzonite did not form by the mixing of ferrodiorite with monzosyenite, which could otherwise explain many of the major- and trace-element characteristics of the fine-grained monzonite, including the shape of REE patterns (Kolker et al., 1988). Fine-grained monzonite has a more evolved major- and trace-element chemistry than that of ferrodiorite, but Sr and Nd isotopic data require a source that is isotopically more primitive than the source of the anorthosite-ferrodiorite series. Because initial Sr isotope ratios of fine-grained monzonite are less radiogenic than ferrodiorite, it is unlikely that fine-grained monzonite formed by contamination of ferrodiorite with lower Proterozoic country rock inclusions or melts. Initial Sr and Nd isotopic ratios for fine-grained monzonite are intermediate between monzosyenite and biotite gabbro (Table 2); magma- or source-mixing between monzosyenite and biotite gabbro are not, however, supported by major- and trace-element data (Fig. 9; Kolker, 1989).

Depleted-mantle Nd model ages for Maloin Ranch fine-grained monzonite (1795 Ma; 1816 Ma; Kolker, 1989) are consistent with melting of mantle-derived mafic material added to the Wyoming Craton at about 1.8 Ga (DePaolo, 1981; Condie and Shadel, 1984; Nelson and DePaolo, 1984, 1985; Reed et al., 1987; Geist et al., 1989). Because DePaolo (1981) used Nd isotope data for arc magmas of the northern Colorado Province to define his depleted-mantle model curve at 1.8 Ga, T_{dm} for fine-grained monzonite calculated in this manner should coincide with the age of the underplated magmas, if older crustal contaminants have not been added.

Whereas various workers favor a lower-crustal source for fine-grained monzonite equivalents at anorthosite margins (Duchesne et al., 1985a, 1985b, 1989; McLelland, 1988), uncertainty regarding the composition of the lower crust, conditions of melting, and residual mineralogy has limited the development of quantitative models. Duchesne et al. (1985b) suggested an oxide-rich noritic cumulate as the lower-crustal precursor for monzonitic dikes in the Egersund-Ogna anorthosite of the Rogaland Complex. This source seems unlikely because of its probable limited extent and its compositional similarity to the proposed melt.

Compositions of lower-crustal xenoliths in Colorado-Wyoming Province kimberlites indicate that the underlying crust approximates a continental tholeiite (Bradley and McCallum, 1984), similar to model compositions for the lower crust (e.g., Taylor and McLennan, 1985) and averages from other xenolith suites (e.g., Rudnick and Taylor, 1987). Sm-Nd dating of two granulitic xenoliths

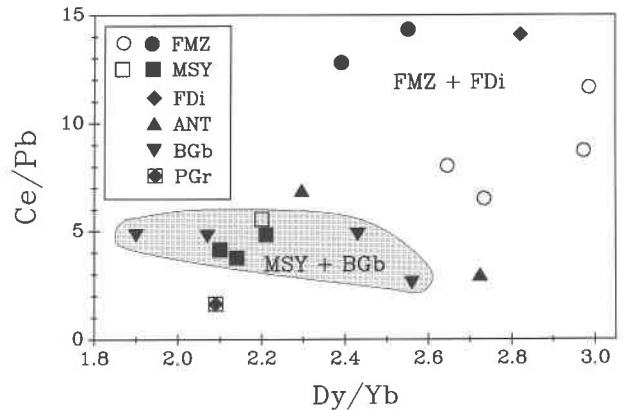


Fig. 9. Incompatible-element ratio-ratio plot (Langmuir et al., 1978) showing fine-grained monzonite data (circles) relative to data for monzosyenite (squares) and biotite gabbro (inverted triangles) shown in shaded field. Fine-grained monzonite ratios should fit a mixing curve (not shown) between monzosyenite and biotite gabbro if the fine-grained monzonite is related to these end-members by magma mixing or mixing of sources, which would be consistent with isotopic data alone (Kolker, 1989). Open symbols = Sybille; filled symbols = Maloin Ranch; PGr = porphyritic granite; other symbols as indicated.

in a Colorado-Wyoming kimberlite (DePaolo, 1981) suggests that mantle-derived 1.8-Ga material is present at depth. Seismic reflection and refraction studies indicate present depths to the Moho ranging from about 40 km (Gohl et al., 1988) to nearly 50 km (Allmendinger et al., 1982) along traverses that transect the Laramie Complex. Assuming the Maloin Ranch monzosyenite was emplaced at 4.0–4.5 kbar (Kolker and Lindsley, 1989), pressures at the base of the crust could have been as high as 15–18 kbar at 1.4 Ga. Geobarometry of lower-crustal xenoliths (Bradley and McCallum, 1984) indicates these equilibrated at pressures of 10–15 kbar.

Melting experiments on basaltic compositions may help evaluate a mafic lower-crustal source for fine-grained monzonite, but experiments at the appropriate conditions (10–18 kbar, very low H_2O) are limited. Most studies have been conducted under water-saturated conditions. Despite that fact, it is clear that small to moderate amounts of melting of basalt will give an appropriate Mg number of about 0.25 at a large range of pressures and water fugacities (Green and Ringwood, 1968; Helz, 1976; Holloway and Burnham, 1972; Stern and Wyllie, 1973; Spulber and Rutherford, 1983). Dry melting of a quartz tholeiite at 18 kbar (Green and Ringwood, 1968) shows enrichment in alkalis and a low Mg number without extensive silica enrichment. At 35% melting, K_2O of the melt is enriched by a factor of 2.7, close to the incompatible limit of 2.9 at $f = 0.35$. The Mg number of this melt is 0.28, and the residue is dominated by clinopyroxene.

Baker and Eggler (1987) melted a range of basaltic and andesitic compositions under dry conditions at 1 atm and

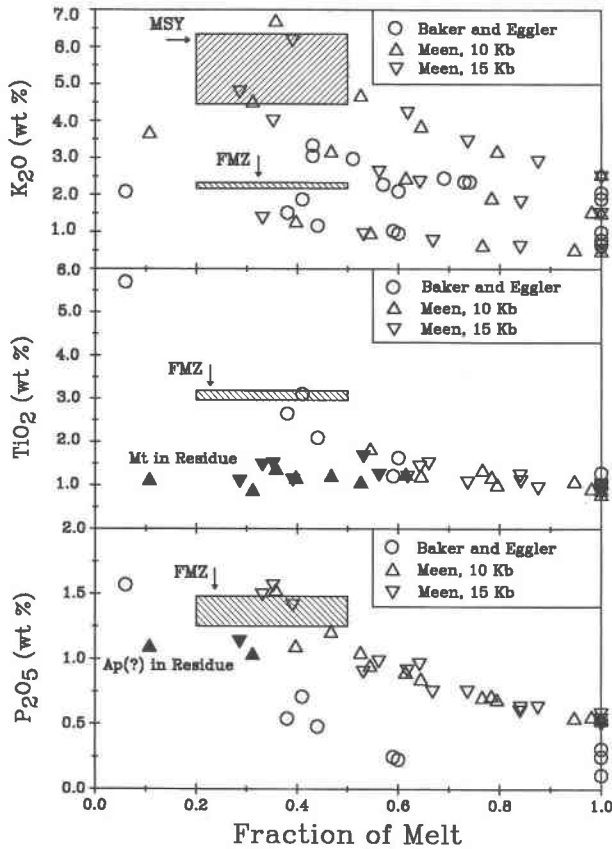


Fig. 10. Variation of K_2O , P_2O_5 , and TiO_2 with fraction of melting in basalt melting experiments at 8 kbar of Baker and Eggler (1987) and at 10 and 15 kbar (Meen, 1990), compared to values for Maloin Ranch rocks. Solid symbols indicate presence of magnetite or apatite in the residue at high fO_2 , limiting enrichment of TiO_2 or P_2O_5 , (respectively) for a given fraction of melt. Data suggest low to moderate amounts of melting of basalt (fraction of melt of about 0.2 to 0.5) are required for enrichments of P_2O_5 , TiO_2 , and K_2O in Maloin Ranch fine-grained monzonite, the range for which is indicated by the thickness of bar in each diagram.

8 kbar. As noted by Duchesne et al. (1989), these experiments show that enrichment in TiO_2 and P_2O_5 , characteristic features of both ferrodiorite and fine-grained monzonite, accompanies enrichment in incompatible elements at low to intermediate fractions of melting (Fig. 10). The experiments of Baker and Eggler are under graphite-saturated conditions, consistent with the low fO_2 inferred for fine-grained monzonite and monzosyenite (Kolker and Lindsley, 1989). At high fO_2 , the presence of Fe-Ti oxides and apatite in the residue limits Ti- and P-enrichment of the melt for small amounts of melting (Meen, 1990; Fig. 10).

To further test the basalt-melting model for fine-grained monzonite, we use a plot of Ce versus Zr (Fig. 11). These elements are similarly incompatible, and their ratio should therefore remain relatively constant during processes such

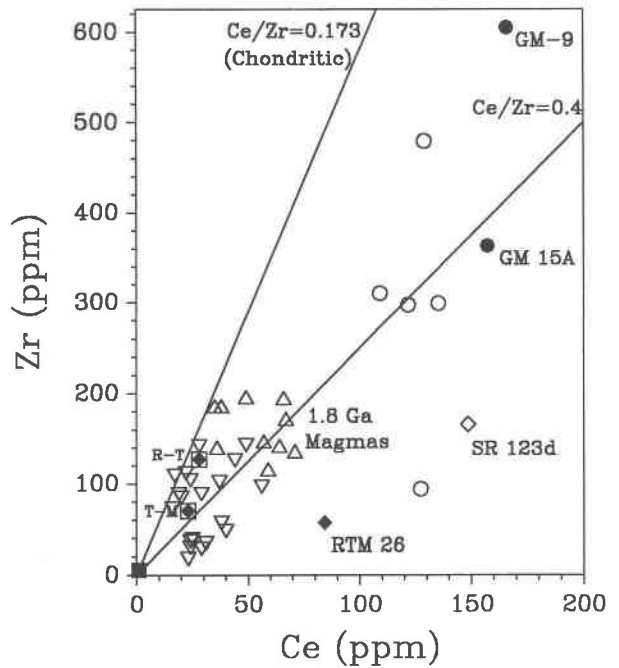


Fig. 11. Plot of Ce versus Zr for Maloin Ranch and Sybille fine-grained monzonite (solid and open circles, respectively) and ferrodiorite (solid and open diamonds). Ce content of Sybille ferrodiorite SR 123d is estimated from its Nd concentration (96.3 ppm; Kolker, 1989), assuming a Ce/Nd of 1.54, as in RTM 26. Also shown are data for ca. 1.8-Ga mafic (inverted triangle) and felsic (triangle) arc magmas of the Colorado Province, including the Green Mountain group of southeastern Wyoming (Condie and Shadel, 1984) and the Dubois Greenstone of west-central Colorado (Condie and Nuter, 1981). Lower crustal averages (diamond in box) by Taylor and McLennan (1985; T-M) and Rudnick and Taylor (1987; R-T) are shown for reference. See text for interpretation.

as melting or fractionation for rocks that approximate liquids (as is likely for ferrodiorite and fine-grained monzonite). Zr can be treated as a trace element in these rocks because they are not zircon-saturated at magmatic temperatures (Kolker and Lindsley, 1989; Watson and Harrison, 1983). Also shown in Figure 11 are Ce and Zr data for mantle-derived 1.8-Ga arc magmas from the Colorado Province (Condie and Nuter, 1981; Condie and Shadel, 1984), representing the lower crust south of the Cheyenne Belt.

Ce and Zr data for the fine-grained monzonite and the 1.8-Ga arc magmas scatter about a line that intersects the origin and has a Ce/Zr of about 0.4 (Fig. 11). This array suggests that the fine-grained monzonite is derived from the same source as the arc magmas (i.e., the mantle at 1.8 Ga) but requires that the Ce/Zr ratio has not changed by fractionation or subsequent melting events. Data for one Maloin Ranch fine-grained monzonite (GM 9) plots well above the Ce/Zr reference line, but its high Zr content can be attributed to inclusion of zircon from the monzosyenite (Kolker and Lindsley, 1989; Fig. 5). Of the

incompatible elements determined for fine-grained monzonite, K, Ce, Zr, and Nb ratios are generally within the range of model lower-crustal values (Taylor and McLennan, 1985; Rudnick and Taylor, 1987). Rb and Pb are, however, relatively depleted, suggesting that the source of the fine-grained monzonite may be somewhat depleted in Rb and Pb, relative to the other incompatible elements.

Maloin Ranch ferrodiorite (RTM 26) plots well below the $Ce/Zr = 0.4$ lower-crust reference line in Figure 11, having a Ce/Zr of 1.48. Incompatible element concentrations are higher for the Sybille ferrodiorite (SR 123d), but it also plots well below the reference line (estimated $Ce/Zr = 0.9$). Within the restrictions of the model, Ce and Zr data for the ferrodiorites again suggest that they are not derived by partial melting of mafic lower crust.

Maloin Ranch fine-grained monzonite is enriched in the REE relative to Sybille fine-grained monzonite. Because the Mg number of Maloin Ranch fine-grained monzonite is higher than that of Sybille, this enrichment cannot be explained by smaller amounts of melting of a similar source, and probably not by larger amounts of fractionation (unless apatite is involved). The data would therefore suggest differences in REE content, but similar LREE enrichment, for the sources of Maloin Ranch and Sybille fine-grained monzonite.

Origin of monzosyenite

Viable models for monzosyenite petrogenesis must explain the extreme enrichment in alkalis and incompatible elements, the lack of silica enrichment, and the very low Mg number. Arguments similar to those presented for fine-grained monzonite suggest the source of the monzosyenite is independent of the anorthositic rocks. Major- and trace-element data suggest a more evolved source than that of the fine-grained monzonite, as enrichment in K_2O and certain incompatible elements and a low Mg number (0.10–0.16) would require very small amounts of melting of a purely basaltic lower crust.

REE patterns for fine-grained monzonite and monzosyenite show similar LREE enrichment, but the characteristic HREE flattening shown by monzosyenite may indicate differences in mineralogy of the source or residue (i.e., presence of garnet) versus that of fine-grained monzonite. Isotopic data for monzosyenite are consistent with a dominant 1.7–1.8-Ga source component, but would also require smaller amounts of an older (lower Proterozoic) source component, evident in Nd, Sr, and Pb isotopic data (Kolker, 1989).

Melting experiments provide limited constraints for monzosyenite petrogenesis. Ternary relations in the granite system require a substantially thickened crust (consistent with seismic profiles) for a quartz-saturated monzosyenite magma (Wyllie, 1977). Mineralogy and geothermometry of syenitic rocks indicate that the melts must have been produced under relatively dry conditions, with minimum emplacement temperatures of 900–950 °C (Fuhrman et al., 1988; Kolker and Lindsley, 1989).

A rhyolite melted with 5% H_2O at 15 kbar (Huang and Wyllie, 1986) yielded liquids less siliceous than the starting material, showing some characteristics of syenites but at temperatures of only 650–700 °C. Compared to 1 atm experiments, fractionation of basalt at 10 kb leads to much greater enrichment in K_2O for a given SiO_2 content (Meen, 1987; Meen, 1990). Melting of such an evolved source may explain the K_2O -enrichment of monzosyenite. Some characteristics of syenitic rocks are also evident in intermediate (~50%) melt fractions of the more evolved (andesitic) compositions studied by Baker and Eggler (1987; Fig. 10).

DISCUSSION

The ferrodiorite-to-granite continuum at anorthosite margins is difficult to explain by a single process, such as fractionation, melting, or mixing. In the Maloin Ranch pluton, it is likely that all of these processes played a role in explaining the observed compositional diversity. That partial melting of mafic lower crust can produce magmas such as the fine-grained monzonite with major- and trace-element characteristics similar to those expected for anorthosite residual liquids may help explain the persisting petrogenetic controversy.

The variable europium anomalies observed in fine-grained monzonite and equivalent rocks can be explained by variation in the proportion of plagioclase to clinopyroxene in the residual assemblage. Because strongly negative europium anomalies are uncommon, a pyroxene-dominated residue is inferred, consistent with some melting experiments on mafic compositions (e.g., Green and Ringwood, 1968; Huang and Wyllie, 1986). The experiments of Baker and Eggler (1987) contain larger proportions of plagioclase in the residue but are useful in illustrating how P_2O_5 and TiO_2 may become enriched in the melt in the absence of residual Fe-Ti oxides and apatite.

Derivation of fine-grained monzonite by melting at depth requires a LREE-enriched lower crust that has not been depleted (in REE) by previous melting events. REE analyses of several lower crustal xenoliths from the Colorado-Wyoming district (M. E. McCallum, unpublished data) are consistent with these requirements, but the xenoliths may not be a representative sampling. With the exception of a Sybille fine-grained monzonite (sample LAC 6A), isotopic data do not require an Archean component at depth, consistent with the tectonic model of Geist et al. (1989), in which the 1.7–1.8 Ga basement terrane was accreted to the margin of the Wyoming craton along a subduction zone having a north-dipping component.

SUMMARY AND CONCLUSIONS

Field, geochemical, and isotopic data are most consistent with a comagmatic relation between anorthositic rocks and ferrodiorite, either by fractionation or immiscibility. If ferrodiorite is a residual liquid by fractiona-

tion, plagioclase-melt distribution coefficients for K and Rb must be higher than published values.

Major-element, trace-element and isotopic characteristics of fine-grained monzonite and monzosyenite are best explained by low to moderate amounts of melting of mafic and intermediate materials in a thickened (~50 km) lower crust, at dry conditions. Melting of mantle-derived basaltic material added to the Wyoming craton at 1.7–1.8 Ga is the most likely source for the fine-grained monzonite. Incompatible element ratios for fine-grained monzonite suggest its lower-crustal source was depleted in some incompatible elements, consistent with a deep-crustal history. Trace-element data and isotopic analyses for the monzosyenite are consistent with a more evolved source or more extensive fractionation history, compared to the fine-grained monzonite. Modal mineralogy, REE patterns, and covariation of trace-element data with Eu anomaly show that most monzosyenites are feldspar cumulates, but the proportion of liquid is highly variable.

REE data reflect a diverse history for the range of granitic rocks in the Maloin pluton. Maloin Ranch porphyritic granite generally grades into a rock like that of Sherman Granite, but the REE pattern of one porphyritic segregation (sample RTM 56) suggests it is independent of the adjacent body of Sherman Granite. Maloin Ranch granitic dikes reflect late-stage mobility of felsic melts with varying fluid contents. Some aplites (e.g., sample RTM 32) appear to be derived by partial melting of lower Proterozoic pelitic country rocks.

ACKNOWLEDGMENTS

We thank J.-C. Duchesne for pointing out the experiments of Baker and Egger and their implications for the evolved series. We are grateful to M. E. McCallum, J. K. Meen, and R. E. Zartman for making their unpublished data available to us. Discussions with I. C. Anderson, O. C. Evans, B. R. Frost, C. D. Frost, D. J. Geist, J. A. Grant, E. J. Krogstad, K. Mezger, S. A. Morse, H. Nekvasil, E. C. Simmons, and R. A. Wiebe have been most helpful. Initial reviews by S. M. McLennan, H. Nekvasil, and R. A. Wiebe helped improve the manuscript, as did a subsequent review by L. P. Gromet. This study was funded by NSF grant EAR-8618480 to D. H. Lindsley, and EAR-8617812 to B. R. Frost and C. D. Frost. The Stony Brook isotope geochemistry lab was supported by NSF grant EAR-8607973 to G. N. Hanson during acquisition of REE data.

REFERENCES CITED

- Aleinikoff, J.N. (1983) U-Th-Pb systematics of zircon inclusions in rock-forming minerals: A study of armoring against isotopic loss using the Sherman Granite of Colorado-Wyoming, USA. *Contributions to Mineralogy and Petrology*, 83, 259–269.
- Allmendinger, R.W., Brewer, J.A., Brown, L.D., Kaufman, S., Oliver, J.E., and Houston, R.S. (1982) COCORP profiling across the Rocky Mountain Front in southern Wyoming, Part 2: Precambrian basement structure and its influence on Laramide deformation. *Geological Society of America Bulletin*, 93, 1253–1263.
- Anderson, J.L. (1983) Proterozoic anorogenic plutonism of North America. In L.G. Medaris, Jr. et al., Eds., *Proterozoic geology: Selected papers from an international Proterozoic symposium*. Geological Society of America Memoir 161, 133–154.
- (1987) The origin of A-type Proterozoic magmatism: A model of mantle and crustal overturn. *Geological Society of America Abstracts with Programs*, 19, 7, 571.
- Ashwal, L.D. (1978) Petrogenesis of massif-type anorthosites: Crystallization history and liquid line of descent of the Adirondack and Morin complexes, 136 p. Ph.D. dissertation, Princeton University, Princeton, New Jersey.
- Ashwal, L.D., and Siefert, K.E. (1980) Rare-earth element geochemistry of anorthosite and related rocks from the Adirondacks, New York, and other massif-type complexes. *Geological Society of America Bulletin*, 91, 659–684.
- Ashwal, L.D., and Wooden, J.L. (1983) Sr and Nd isotope geochronology, geologic history, and origin of the Adirondack Anorthosite. *Geochimica et Cosmochimica Acta*, 47, 1875–1885.
- Baker, D.R., and Egger, D.H. (1987) Compositions of anhydrous and hydrous melts coexisting with plagioclase, augite, and olivine or low-Ca pyroxene from 1 atm to 8 kbar: Application to the Aleutian volcanic center of Atka. *American Mineralogist*, 72, 12–28.
- Bradley, S.D., and McCallum, M.E. (1984) Granulite facies and related xenoliths from Colorado-Wyoming kimberlite. In J. Kornprobst, Ed., *Kimberlites, II: The mantle and crust-mantle relationships*, Proceedings of the Third International Kimberlite Conference, v. II, p. 205–217. Elsevier, Amsterdam.
- Carron, J.-P., and Lagache, M. (1980) Etude expérimentale du fractionnement des éléments Rb, Cs, Sr, et Ba entre feldspaths alcalins, solutions hydrothermales et liquides silicatés dans le système Q-Ab-Or-H₂O à 2 kbar entre 700 et 800 °C. *Bulletin de Minéralogie*, 103, 571–578.
- Condie, K.C., and Nuter, J.A. (1981) Geochemistry of the Dubois greenstone succession: An early Proterozoic bimodal volcanic association in west-central Colorado. *Precambrian Research*, 15, 131–155.
- Condie, K.C., and Shadel, C.A. (1984) An early Proterozoic volcanic arc succession in southeastern Wyoming. *Canadian Journal of Earth Science*, 21, 415–427.
- DePaolo, D.J. (1981) Neodymium isotopes in the Colorado Front Range and crust-mantle evolution in the Proterozoic. *Nature*, 291, 5811, 193–196.
- Duchesne, J.-C. (1984) Massif anorthosites: Another partisan review. In W.L. Brown, Ed., *Feldspars and feldspathoids*, p. 411–433. Reidel, Boston.
- Duchesne, J.-C., Maquil, R., and Demaiffe, D. (1985a) The Rogaland anorthosites: Facts and speculations. In A.C. Tobi and J.L.R. Touret, Eds., *The deep Proterozoic crust in the North Atlantic provinces*, p. 449–476. Reidel, Boston.
- Duchesne, J.-C., Roelandts, I., Demaiffe, D., and Weis, D. (1985b) Petrogenesis of monzonitic dykes in the Egersund-Ogna anorthosite (Rogaland, S.W. Norway): Trace elements and isotopic (Sr, Pb) constraints. *Contributions to Mineralogy and Petrology*, 90, 214–225.
- Duchesne, J.-C., Wilmart, E., Demaiffe, D., and Hertogen, J. (1989) Monzonites from Rogaland (southwest Norway): A series of rocks coeval but not comagmatic with massif-type anorthosites. *Precambrian Research*, 45, 111–128.
- Duebendorfer, E.M., and Houston, R.S. (1987) Proterozoic accretionary tectonics of the southern margin of the Archean Wyoming craton. *Geological Society of America Bulletin*, 98, 554–568.
- Ellison, A.J.G., and Hess, P.C. (1989) Solution properties of rare earth elements in silicate melts: Inferences from immiscible liquids. *Geochimica et Cosmochimica Acta*, 53, 1965–1974.
- Emslie, R.F. (1980) Geology and petrology of the Harp Lake Complex, central Labrador: An example of Elsonian magmatism. 136 p. Geological Survey of Canada Bulletin.
- (1985) Proterozoic anorthosite massifs. In A.C. Tobi and J.L.R. Touret, Eds., *The deep Proterozoic crust in the North Atlantic provinces*, p. 39–60. Reidel, Boston.
- Epler, N.A. (1987) Experimental study of Fe-Ti oxide ores from the Sybille Pit in the Laramie Anorthosite, Wyoming, 67 p. M.S. thesis, State University of New York, Stony Brook, New York.
- Evans, O.C. (1987) The petrogenesis of the Saganaga Tonalite revisited, 97 p. M.S. thesis, State University of New York, Stony Brook, New York.
- Flynn, R.T., and Burnham, C. Wayne (1978) An experimental determination of rare earth partition coefficients between a chloride containing vapor phase and silicate melts. *Geochimica et Cosmochimica Acta*, 42, 685–701.

- Fountain, J.C., Hodge, D., and Hills, F.A. (1981) Geochemistry and petrogenesis of the Laramie Anorthosite Complex. *Lithos*, 14, 113–132.
- Frost, C.D., Meier, M., and Oberli, F. (1990) Single crystal U-Pb zircon age determination of the Red Mountain pluton, Laramie Anorthosite Complex. *American Mineralogist*, 75, 21–26.
- Fuhrman, M.L., Frost, B.R., and Lindsley, D.H. (1988) Crystallization conditions of the Sybille monzosyenite, Laramie Anorthosite Complex, Wyoming. *Journal of Petrology*, 29, 699–729.
- Geist, D.J., Frost, C.D., Kolker, Allan, and Frost, B.R. (1989) A geochemical study of magmatism across a major terrane boundary: Sr and Nd isotopes in Proterozoic granitoids of the southern Laramie Range, Wyoming. *Journal of Geology*, 97, 331–342.
- Geist, D.J., Frost, C.D., and Kolker, Allan (1990) Sr and Nd isotopic constraints on the origin of the Laramie Anorthosite Complex, Wyoming. *American Mineralogist*, 75, 13–20.
- Gill, J.B., and Murthy, V.R. (1970) Distribution of K, Rb, Sr and Ba in Nain anorthosite plagioclase. *Geochimica et Cosmochimica Acta*, 34, 401–408.
- Gohl, K., May, M.T., Carbonell, R., Speece, M.A., Hawman, R.B., and Smithson, S.B. (1988) Wide-angle reflection studies in the Laramie Range, Wyoming: Preliminary results. *EOS*, 69, 406.
- Goldberg, S.A. (1984) Geochemical relationships between anorthosite and associated iron-rich rocks, Laramie Range, Wyoming. *Contributions to Mineralogy and Petrology*, 87, 376–387.
- Green, T.H., and Ringwood, A.E. (1968) Genesis of the calc-alkaline igneous rock suite. *Contributions to Mineralogy and Petrology*, 18, 105–162.
- Hanson, G.N. (1980) Rare earth elements in petrogenetic studies of igneous systems. *Annual Review of Earth and Planetary Sciences*, 8, 371–406.
- Harrison, T.M., and Watson, E.B. (1984) The behavior of apatite during crustal anatexis: Equilibrium and kinetic considerations. *Geochimica et Cosmochimica Acta*, 48, 1467–1477.
- Helz, R.T. (1976) Phase relations of basalts in their melting ranges at $p_{H_2O} = 5$ kb. Part II. Melt compositions. *Journal of Petrology*, 17, 139–193.
- Hills, F.A., and Houston, R.A. (1979) Early Proterozoic tectonics of the central Rocky Mountains, North America. *Contributions to Geology, University of Wyoming*, 17, 89–109.
- Holloway, J.R., and Burnham, C. Wayne (1972) Melting relations of basalt with equilibrium water pressure less than total pressure. *Journal of Petrology*, 13, 1–29.
- Huang, W.-L., and Wyllie, P.J. (1986) Phase relationships of gabbro-tonalite-granite-water at 15 kbar with applications to differentiation and anatexis. *American Mineralogist*, 71, 301–316.
- Karlstrom, K.E., and Houston, R.S. (1984) The Cheyenne Belt: Analysis of a Proterozoic suture in southern Wyoming. *Precambrian Research*, 25, 415–446.
- Kolker, Allan (1989) Petrology and geochemical evolution of the Maloin Ranch pluton, Laramie Anorthosite Complex, Wyoming; 211 p. Ph.D. dissertation, State University of New York, Stony Brook, New York.
- Kolker, Allan, and Lindsley, D.H. (1989) Geochemical evolution of the Maloin Ranch pluton, Laramie Anorthosite Complex, Wyoming: Petrology and mixing relations. *American Mineralogist*, 74, 307–324.
- Kolker, Allan, Lindsley, D.H., and Geist, D.J. (1988) Fractionation(?), mixing and assimilation in the Maloin Ranch pluton, Laramie Anorthosite Complex, Wyoming (abs.). *EOS*, 69, 513.
- Langmuir, C.H., Vocke, R.D., Hanson, G.N., and Hart, S.R. (1978) A general mixing equation with applications to Icelandic basalts. *Earth and Planetary Science Letters*, 37, 380–392.
- Luth, W.C., Jahns, R.H., and Tuttle, O.F. (1964) The granite system at pressures of 4 to 10 kilobars. *Journal of Geophysical Research*, 69, 759–773.
- Masuda, A., Nakamura, N., and Tanaka, T. (1973) Fine structures of mutually normalized rare-earth patterns of chondrites. *Geochimica et Cosmochimica Acta*, 37, 239–248.
- Masuda, A., Kawakami, O., Dohmoto, Y., and Takenaka, T. (1987) Lanthanide tetrad effects in nature: Two mutually opposite types, W and M. *Geochemical Journal*, 21, 119–124.
- McLelland, J.M. (1988) Mid to Late Proterozoic magmatism within northeastern North America and its implications for the growth of the continental crust. In L.D. Ashwal, Ed., *Workshop on the growth of the continental crust*. LPI Technical Report 88-02, 101–102.
- Meen, J.K. (1987) Formation of shoshonites from calcalkaline basalt magmas: Geochemical and experimental constraints from the type locality. *Contributions to Mineralogy and Petrology*, 97, 333–351.
- Meen, J.K. (1990) Elevation of potassium content of basaltic magma by fractional crystallization: The effect of pressure. *Contributions to Mineralogy and Petrology*, 104, 309–331.
- Mineyev, D.A. (1963) Geochemical differentiation of the rare earths. *Geochemistry (U.S.S.R.)*, 1129–1149.
- Morse, S.A. (1981) Kiglapait geochemistry III: Potassium and rubidium. *Geochimica et Cosmochimica Acta*, 45, 163–180.
- (1982) A partisan review of Proterozoic anorthosites. *American Mineralogist*, 67, 1087–1100.
- Morse, S.A., and Nolan, K.M. (1985) Kiglapait geochemistry VII: Yttrium and the rare earth elements. *Geochimica et Cosmochimica Acta*, 49, 1621–1644.
- Nekvasil, Hanna (1988) Calculated effect of anorthite component on the crystallization paths of H_2O -undersaturated haplogranitic melts. *American Mineralogist*, 73, 966–981.
- Nekvasil, Hanna, and Burnham, C.W. (1987) The individual effects of pressure and water content on phase equilibria in the “granite system.” In *Magmatic processes: Physicochemical principles*, p. 433–445. *Geochemical Society Special Publication* 1.
- Nelson, B.K., and DePaolo, D.J. (1984) 1,700-Myr greenstone volcanic successions in southwestern North America and isotopic evolution of the Proterozoic mantle. *Nature*, 312, 143–146.
- (1985) Rapid production of continental crust 1.7–1.9 b.y. ago: Nd isotopic evidence from the basement of the North American mid-continent. *Geological Society of America Bulletin*, 96, 746–754.
- Norrish, K., and Hutton, J.T. (1969) An accurate X-ray spectrographic method for the analysis of a wide range of geological samples. *Geochimica et Cosmochimica Acta*, 33, 431–453.
- Norrish, K., and Chappell, B.W. (1977) X-ray fluorescence spectrometry. In J. Zussman, Ed., *Physical methods in determinative mineralogy* (2nd edition), p. 201–272. Academic Press, New York.
- Philpotts, A.R. (1966) Origin of the anorthosite-mangerite rocks in Southern Quebec. *Journal of Petrology*, 7, 1–64.
- (1982) Compositions of immiscible liquids in volcanic rocks. *Contributions to Mineralogy and Petrology*, 80, 201–218.
- Philpotts, J.A., and Schnetzler, C.C. (1970) Phenocryst-matrix partition coefficients for K, Rb, Sr and Ba, with applications to anorthosite and basalt genesis. *Geochimica et Cosmochimica Acta*, 34, 307–322.
- Reed, J.C., Jr., Bickford, M.E., Premo, W.R., Aleinikoff, J.N., and Palister, J.S. (1987) Evolution of the Early Proterozoic Colorado province: Constraints from U-Pb geochronology. *Geology*, 15, 861–865.
- Roedder, Edwin (1951) Low temperature liquid immiscibility in the system $K_2O-FeO-Al_2O_3-SiO_2$. *American Mineralogist*, 36, 282–286.
- (1978) Silicate liquid immiscibility in magmas and in the system $K_2O-FeO-Al_2O_3-SiO_2$: An example of serendipity. *Geochimica et Cosmochimica Acta*, 42, 1597–1617.
- Rudnick, R.L., and Taylor, S.R. (1987) The composition and petrogenesis of the lower crust: A xenolith study. *Journal of Geophysical Research*, 92, 13981–14005.
- Ryerson, F.J., and Hess, P.C. (1978) Implications of liquid-liquid distribution coefficients to mineral-liquid partitioning. *Geochimica et Cosmochimica Acta*, 42, 921–932.
- (1980) The role of P_2O_5 in silicate melts. *Geochimica et Cosmochimica Acta*, 44, 611–624.
- Shirey, S.B. (1984) The origin of Archean crust in the Rainy Lake area, Ontario, 393 p. Ph.D. dissertation, State University of New York, Stony Brook, New York.
- Shirey, S.B., and Hanson, G.N. (1986) Mantle heterogeneity and crustal recycling in Archean granite-greenstone belts: Evidence from Nd isotopes and trace elements in the Rainy Lake area, Superior Province, Ontario, Canada. *Geochimica et Cosmochimica Acta*, 50, 2631–2651.
- Simmons, E.C., and Hanson, G.N. (1978) Geochemistry and origin of massif-type anorthosites. *Contributions to Mineralogy and Petrology*, 66, 119–135.

- Spulber, S.D., and Rutherford, M.J. (1983) The origin of plagiogranite in oceanic crust: An experimental study. *Journal of Petrology*, 24, 1–25.
- Stern, C.R., and Wyllie, P.J. (1973) Melting relations of basalt-andesite-rhyolite-H₂O and a pelagic red clay at 30 kilobars. *Contributions to Mineralogy and Petrology*, 42, 313–323.
- Subbarayudu, G.V., Hills, F.A., and Zartman, R.E. (1975) Age and Sr isotopic evidence for the origin of the Laramie anorthosite-syenite complex, Laramie Range, Wyoming. *Geological Society of America Abstracts with Programs*, 7, 1287.
- Taylor, S.R., and McLennan, S.M. (1985) *The continental crust: Its composition and evolution*, 312 p. Blackwell Scientific Publications, Oxford.
- Vocke, R.D., Jr. (1983) Petrogenetic modelling in an Archean gneiss terrain, Saglek, northern Labrador, 273 p. Ph.D. dissertation, State University of New York, Stony Brook, New York.
- Watson, E.B. (1976) Two-liquid partition coefficients: Experimental data and geochemical implications. *Contributions to Mineralogy and Petrology*, 56, 119–134.
- Watson, E.B., and Harrison, T.M. (1983) Zircon saturation revisited: Temperature and composition effects in a variety of crustal magma types. *Earth and Planetary Science Letters*, 64, 295–304.
- Wiebe, R.A. (1979) Fractionation and liquid immiscibility in an anorthositic pluton of the Nain Complex, Labrador. *Journal of Petrology*, 20, 239–269.
- (1980) Anorthositic magmas and the origin of Proterozoic anorthosite massifs. *Nature*, 286, 564–567.
- (1984) Commingling of magmas in the Bjerkrem-Sogndal lopolith (southwest Norway): Evidence for the composition of residual liquids. *Lithos*, 17, 171–188.
- Wiebe, R.A., and Wild, T. (1983) Fractional crystallization and magma mixing in the Tugalak layered intrusion, the Nain anorthosite complex, Labrador. *Contributions to Mineralogy and Petrology*, 84, 327–344.
- Wyllie, P. J. (1977) Crustal anatexis: An experimental review. *Tectonophysics*, 13, 41–71.

MANUSCRIPT RECEIVED MAY 5, 1989

MANUSCRIPT ACCEPTED JANUARY 20, 1990